TISSUE ENGINEERING: Part A
Volume 17, Numbers 21 and 22, 2011

DOI: 10.1089/ten.tea.2010.0685

The Interplay Between Cell Adhesion Cues and Curvature of Cell Adherent Alginate Microgels in Multipotent Stem Cell Culture

John J. Schmidt, M.S.,[1,2] Jaehyun Jeong, Ph.D.,[1,2] and Hyunjoon Kong, Ph.D.[1,2]

Cell-adherent microcarriers are increasingly used to expand multipotent stem cells on a large scale for therapeutic applications. However, the role of the microcarrier properties and geometry on the phenotypic activities of multipotent cells has not been well studied. This study presents a significant interplay of the number of cell adhesion sites and the curvature of the microcarrier in regulating cell growth and differentiation by culturing mesenchymal stem cells on alginate microgels chemically linked with oligopeptides containing the Arg-Gly-Asp (RGD) sequence. Interestingly, the cell growth rate and osteogenic differentiation level were increased with the RGD peptide density. At a given RGD peptide density, the cell growth rate was inversely related to the microgel diameter, whereas the osteogenic differentiation level was minimally influenced. The dependency of the cell growth rate on the microgel diameter was related to changes in shear stresses acting on cells according to simulation. Overall, this study identifies material variables key to regulating cellular activities on microcarriers, and these findings will be useful to designing a broad array of bioactive microcarriers.

Introduction

Various multipotent cells that include stem and progenitor cells are being studied for the treatments of chronic diseases and tissue defects.[1–7] For example, bone marrow-derived cells are commonly being transplanted to reconstitute the immune system of patients with acute leukemia.[8] Cells that secrete therapeutic proteins such as dopamine and vascular endothelial growth factor are also used to treat chronic diseases, including Parkinson's disease or ischemia.[9,10] Multipotent stem and progenitor cells provide versatility in regenerating a wide-array of tissues damaged or lost due to an injury or a disease.[11,12] As many cell therapies are transitioned from the laboratory to the clinic, it is becoming clear that a large number of cells are required to effectively treat a disease or tissue defect.[13]

However, it is challenging to expand cells to the number required for clinical treatments using conventional tissue culture flasks because of the limited surface area for cell adhesion per the flask volume.[14] To sufficiently expand cell populations in a practical amount of space, culturing cells on cell adherent microcarriers suspended in a bioreactor has increased in popularity. Microcarriers of dextran and collagen-coated dextran are commercially available for culturing cells on a large-scale. In recent years, new microcarriers composed of a variety of materials, including agar, gelatin, poly(lactic acid-co-glycolic acid), and bioactive glass have been investigated.[14–18]

Recent studies reported that cell adhesion matrix properties such as the spatial organization of cell adhesion molecules and mechanical stiffness play significant roles in regulating multipotent cell function.[19–21] It is conceivable that these properties of the microcarriers would also influence the diverse activities of multipotent cells while being cultured in a bioreactor. In addition, the curvature of spherical microcarriers presents the potential to affect cellular activities through changes in the shear stress on cells in a bioreactor.[22] Though, limited efforts have been made to define the role of microcarrier properties and geometry on controlling multipotent cell function.[23,24]

This study presents, for the first time, the combined effects of the density of cell adhesion molecules and the diameter of the microcarrier on the proliferation and osteogenic differentiation of multipotent cells. We used a micro-sized alginate hydrogel bead (i.e., alginate microgel) as a model cell-adherent microcarrier. To derive the cell adhesion to the microgel via specific integrin-ligand engagement, alginate was chemically linked with synthetic oligopeptides containing the Arg-Gly-Asp (RGD) sequence (RGD peptides). The number of RGD peptides presented on the hydrogel bead was varied by altering the ratio of unmodified alginate to the alginate linked with RGD peptides, termed as RGD-alginate.

[1]Department of Chemical and Biomolecular Engineering and [2]Institute for Genomic Biology, University of Illinois at Urbana-Champaign, Urbana, Illinois.

The hydrogel bead diameter was also varied at a constant ratio of unmodified alginate and RGD-alginate from 0.5 to 3 mm. Bone marrow-derived mesenchymal stem cells (MSCs) were used to test the role of microcarrier properties in regulating the cell proliferation and differentiation. Thus, this study serves to define microcarrier variables potentially useful for large scale multipotent cell culture.

Materials and Methods

Preparation of cell adherent alginate microgels

Sodium alginate (M_w ~250,000 g/mol) was obtained from FMC Biopolymer. Using previously described carbodiimide chemistry, $(Gly)_4$-Arg-Gly-Asp-Ala-Ser-Ser-Lys (G_4RGDASSKY) oligopeptides (Peptides International), termed as RGD peptides, were covalently linked to the alginate molecules, as previously described.[25] Briefly, an alginate solution was mixed with *N*-hydroxysulfosuccinimide (Pierce), 1-ethyl-3-dimethylaminopropyl) carbodiimide (Pierce), and the oligopeptides. The number ratio between RGD peptides and an alginate chain was kept constant at two oligopeptides to each alginate molecule, according to a radioactive assay conducted in a previous study.[25] Separately for observation purposes, 5-(aminomethyl) fluorescein (Invitrogen) was linked to the alginate molecule, as previously described.[26] Subsequently, the alginate solution was filter sterilized, lyophilized, and reconstituted at 2% (w/v) with Dulbecco's modified Eagle's medium (DMEM; Invitrogen).

To prepare the microgel, alginate was extruded through a capillary tube and dropped into 0.5 M calcium chloride solution (Sigma-Aldrich). Compressed air at varying pressures from 50 to 115 kPa was passed over the capillary tube to alter the diameter of the alginate droplets. Microgels with different densities of cell adhesion peptides were made by mixing unmodified alginate with alginate covalently linked with the RGD peptides, termed as RGD-alginate. Assuming that RGD-alginates are uniformly mixed with the unmodified alginates and the radius of gyration of RGD-alginate, $Rg_{Alginate}$, is the same as that of unmodified alginate, the RGD density on the hydrogel beads, N_{RGD}, was calculated following Equation 1.

$$N_{RGD} = \frac{DS_{RGD}}{\pi(Rg_{Alginate})^2} * \frac{X_{Alginate}}{X_{Alginate}+1} \quad (1)$$

where DS_{RGD} is the number of RGD peptides conjugated to one alginate chain and $X_{Alginate}$ is the ratio of RGD-alginates to unmodified alginate. The microgels were incubated in DMEM before their use with cells, and the medium was exchanged on a daily basis.

Cell culture on the alginate microgel

Mouse clonally derived MSCs (D1 cells; ATCC) with passage number lower than 22 were used in this study. The MSCs were cultured in DMEM (Invitrogen) supplemented with 10% fetal bovine serum (FBS; Invitrogen) and 100 units/mL penicillin–streptomycin (PS; Invitrogen). Cells were suspended with microgels in a 100 mL Cyto-stirred bioreactor (Fisher Scientific) at a density of 1.5×10^5 cells/cm^2 of microgels. The cells were intermittently stirred for 6–8 h to allow the cellular adhesion to the microgel surface. Subsequently, the cells and the microgels were stirred at a rate of 60 RPM in 60 mL of media.

Imaging of cells on microgels

After culture on the microgel, the cells were fixed overnight in 4% paraformaldehyde (Sigma-Aldrich) and washed with phosphate buffer saline (PBS, Invitrogen). The cells were permeabilized with 0.5% Triton X-100 (Sigma-Aldrich) and 5% dry milk in PBS. Intracellular actin stress fibers were stained using Oregon Green 514 phalloidin (Invitrogen). Oregon Green 514 phalloidin was diluted to 5 U/mL in PBS before staining the cells. Alternatively, the cell membranes were stained with octadecyl rhodamine B chloride (Invitrogen) at a concentration of 5 μg/mL overnight. The cells were subsequently washed and observed with a Leica TCS SP2 confocal microscope.

Analysis of cell proliferation

The cell proliferation rate was evaluated by counting the number of cells on alginate microgels on days of 1, 3, 5, and 7. Four populations of microgels were analyzed to calculate the average and standard deviation values. The gels were dissolved with a 50 mM sodium citrate solution to separate the cells from the microgel, and the cells were counted with a hematocytometer. The cell growth rate (k) was quantified with Equation 2:

$$N \Big/ N_0 = 2^{k\cdot 1} \quad (2)$$

where N represents the number of cells present after a length of time in cell culture (t) and N_o represents the number of cells after 1 day of cell culture.

Analysis of osteogenic differentiation

For osteogenic differentiation studies, the MSCs were cultured in DMEM supplemented with 10% FBS (Invitrogen), 100 U/mL PS, 50 μM/mL ascorbic acid (Sigma-Aldrich), 10 mM β-glycerolphosphate (Sigma-Aldrich), and 0.1 μM dexamethasone (Sigma-Aldrich). The osteogenic differentiation level was evaluated with measurements of the osteocalcin and osteopontin secreted by MSCs on day 7 and 14. The secreted osteocalcin and osteopontin were quantified with a Mouse Osteocalcin ELISA kit (Biomedical Technologies) and Osteopontin ELISA kits (R&D Systems), according to the manufacturer's instructions. In short, a sandwich-based ELISA was conducted and the absorbance of the samples was measured at 450 nm using a plate reader (Biotek Instruments).[27] The total amounts of osteocalcin and osteopontin were normalized to the amount of total protein present in each sample, which was characterized with a bicinchoninic acid protein assay (Pierce). Briefly, the cells were collected and lysed using a lysis buffer (Promega). The lysate was reacted with the bicinchoninic acid reagent and the absorbance was read at 562 nm using a UV/Vis photometer (Eppendorf). Eight replicates were measured at each condition. The mineralization of microgel surfaces was observed with von Kossa staining for calcium, and samples were counter-stained with nuclear fast red.

Analysis of chondrogenic differentiation

For chondrogenic differentiation studies, the MSCs were cultured in serum-free DMEM supplemented with 0.1 μM

BMP-2 (Sigma), 0.1 μM dexamethasone (Sigma), 50 μg/mL L-ascorbate-2-phosphate (Sigma), 40 μg/mL L-proline (Sigma), 100 μg/mL sodium pyruvate (Sigma), and ITS-plus (BD Biosciences). The cells were stained with 0.5% Alcian blue (Sigma) and observed. The amount of chondrogenic differentiation by the MSCs on day 14 was evaluated with a guanidine-HCl extraction and measurement of the optical density of the extracted dye at 650 nm with a plate reader.

Evaluation of shear stresses acting on cells using computational fluid dynamics

A computational fluid dynamics (CFD) model was implemented to (i) validate the assumption that microgels in the bioreactor are exposed to relatively uniform shear stress and (ii) calculate the wall shear stresses acting on cells altered with the microgel diameter. Using STAR-CCM commercial CFD tools, the inner volume of the bioreactor was defined with $0.5–2.0 \times 10^6$ computational finite cells depending on the microgel diameter. The moving reference frame model was applied to simulate fluid rotation by impeller. Assuming that the medium was incompressible, turbulent, and Newtonian fluid flow, shear stress, τ, values were estimated by multiplying the symmetric part of the gradient of the velocity field by the dynamic viscosity of the fluid,

$$\tau = v \cdot \left(\frac{1}{2}\right) \cdot (\nabla U + \nabla U^T) \quad (3)$$

where τ is the shear stress tensor, v the experimental dynamic viscosity, and U the three-dimensional (3D) velocity vector. 3D simulations were performed on eight processor workstations, each processor being a 2.67 GHz Intel Xeon CPU with 48GB RAM.

Results

Analysis of alginate microgels

Cell-adherent microgels were prepared by extruding alginate droplets into a calcium chloride solution to crosslink the polymers *in situ*. Fluorescently labeled-alginate microgels were imaged to confirm gelation, and as evident by the low background emission, virtually all of the alginate was incorporated into the microgels (Fig. 1A). In addition, the chemical linkage of RGD peptides with alginate microgel had minimal effects on the microgel morphology and size.

The microgel size was rather significantly affected by the extrusion condition, because the droplets of pre-gelled alginate solution were generated by the compressive pressure of the air around the capillary in which alginate solution flowed. Increasing the air pressure from 50 to 115 kPa decreased the average microgel diameter from 3000 to 300 μm. The diameter of a calcium cross-linked microgel remained constant throughout 1 week of incubation in cell culture medium irrespective of the microgel formulation and air pressure (Fig. 1B).

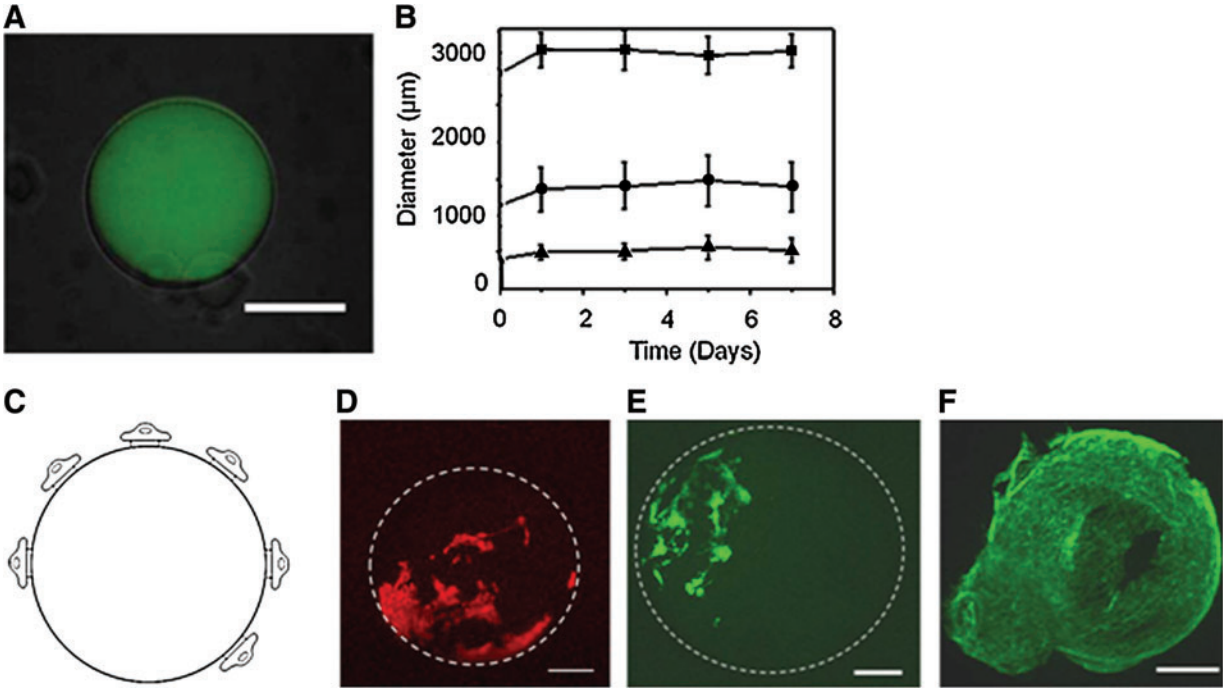

FIG. 1. Characterization of RGD-alginate microgel and MSC culture on the microgel surface **(A)** A fluorescent image of the alginate microgel was superimposed on top of a bright-field image of the same alginate microgel (scale: 300 μm). The alginate microgels were stable in a cell culture media independent of the microgel diameter of 3 mm (■), 1.5 mm (●), and 500 μm (▲). **(B)** The average diameter of alginate microgels was measured using 50 samples per condition. **(C)** Schematic description of cells adhered to a microgel of RGD-alginate. **(D, E)** The cellular membrane **(D)** and intracellular actin **(E)** of MSCs adhered to alginate microgels (marked by a dashed circle) were stained with octadecyl rhodamine B chloride and Oregon green 514 phalloidin, respectively. The image was captured 24 h after seeding MSCs on the microgel beads (Scale bar: 200 μm). The white lines in **(D)** and **(E)** represent the outline of the alginate microgel. **(F)** The cells on the microgels subsequently reached confluency within 10 days (scale: 175 μm). RGD, Arg-Gly-Asp; MSC, mesenchymal stem cell. Color images available online at www.liebertonline.com/tea

Effects of the cell adhesion molecule density of the microgel on cellular activities

MSCs were stirred with the alginate microgels to derive cell adhesion to the microgel surface. As expected, no cells adhered onto alginate microgels devoid of RGD peptides. Instead, cells exclusively adhered to the surface of microgels presenting RGD peptides (Fig. 1C, D). The adhered cells formed stress fibers of intracellular actin filaments, similar to cells adhered onto conventional two-dimensional (2D) cell adhesion substrates (Fig. 1E). After 10 days in culture on the microgel modified with RGD peptide at a density of 6.22×10^8 RGD/mm^2, the cells reached confluency on the microgels (Fig. 1F).

The rate of cellular proliferation on the microgel was tuned with the number of RGD peptides on a microgel. The RGD peptide density of a single microgel (N_{RGD}) was calculated with the ratio between alginate modified with RGD peptides and unmodified alginate, using Equation 1. Increasing N_{RGD} did not significantly affect the number of cells initially adhered to the microgel surface (N_0), but resulted in the increase of cell growth rate calculated using Equation 2 (Fig. 2A, B).

Culturing MSCs adhered to the microgel in the cell growth media did not significantly activate differentiation independent of the type and density of cell adhesion molecule, although there was a slight increase of osteocalcin secretion as the cell density reached confluence (data not shown). However, the MSCs collected from microgels showed the multipotency to differentiate into adipocytes, osteoblasts, or chondrocytes in response to a specific differentiation media (Fig. 2B). MSCs adhered to the microgel at confluency were differentiated into osteogenic lineage when the cell culture medium was supplemented with osteogenic differentiation factors, and the osteogenic differentiation level was mediated by the density of RGD peptides. Increasing N_{RGD} from 6.22×10^7 to 6.22×10^8 RGD/mm^2 increased the cellular secretions of osteocalcin and osteopontin, which are osteogenic differentiation markers (Fig. 2C). Accordingly, the degree of mineralization on microgel surfaces, marked by positive staining of von Kossa reagents, was increased with N_{RGD} (Fig. 2D). Separately, the cells cultured in the media supplemented with chondrogenic differentiation factors also exhibited the larger expression of glycosaminoglycan molecules, positively stained by Alcian blue, with increasing N_{RGD} (Fig. 2E).

Effects of microgel diameter on cell adhesion and proliferation

The effects of the microgel diameter on the cell attachment efficiency and growth rate were examined using RGD-alginate microgels with average diameters of 500, 1500, and 3000 μm. The ratio of unmodified alginate and RGD-alginate was kept constant to present N_{RGD} of the microgels at 6.22×10^8 RGD/mm^2. Therefore, the total RGD peptide number presented from a single microgel was increased with microgel diameter. The increase in the microgel diameter resulted in the increase of the cell attachment efficiency by a factor of three (Fig. 3B). In contrast, the increase of the microgel diameter led to a decrease of the cell growth rate by a factor of four (Fig. 3A, B).

Next, the effect of the microgel diameter on the osteogenic differentiation level was examined by culturing MSCs adhered to the microgel in the osteogenic differentiation media. The density of MSCs initially adhered to the microgel was tuned to be confluent to minimize the role of microgel diameter on the cell growth rate. The cellular secretions of osteocalcin and osteopontin on days 7 were almost independent of the microgel diameter (Fig. 3C).

The cell growth rate and the osteogenic differentiation level were further related to the shear stress acting on the cell, which was calculated by CFD simulation (Fig. 4A). According to the CFD simulation, the entire microgel surfaces in a convective bioreactor were exposed to relatively uniform shear stress. Also, shear stresses acting on the cell increase as the microgel diameter decreases (Fig. 4B-1). Interestingly, the cell growth rate was linearly related to the shear stress altered with the microgel diameter. In contrast, the osteogenic differentiation level was independent of the shear stress (Fig. 4B-2).

To further confirm the relative sensitivity or insensitivity to shear stress, we further exposed the cell-laden microgels of the same diameter (0.5 mm) to different shear stresses by changing the rotational velocity of the microgel. Doubling the calculated shear stress from 0.18 to 0.36 Pa made insignificant changes in cellular secretion of osteopontin (Supplemental Fig. 1; Supplementary Data are available online at www.liebertonline.com/tea).

Discussion

Overall, the results of this study demonstrated the control of cellular function through the combined tuning of the cell adhesion molecule density and geometry of a cell-adherent microcarrier. Alginate microgels displaying varying numbers of chemically linked RGD peptides were prepared by an *in situ* ionic cross-linking reaction. The microgel diameter was varied while keeping the RGD peptide density constant. Alginate microgels modified with RGD peptides were able to derive cell adhesion on the microgel surface, and further tune the cell growth rate and osteogenic differentiation level with the density of the RGD peptides. The cellular activities, specifically cell growth rate, were further regulated by the microgel diameter because of the change of shear stress acting on the cell.

In this study, the alginate microgels were engineered to derive cell adhesion via specific integrin-ligand engagement using chemically linked RGD peptides. It is known that RGD peptides bind with MSC's integrin, $\alpha_5\beta_1$ or $\alpha_V\beta_3$. Therefore, the improvement of MSC's growth rate and osteogenic differentiation level with RGD peptide density should be related to the increase of the number of bonds between cellular integrin and RGD peptides.[20] The quantitative relationship between the RGD peptide density of a microgel and cellular activities agreed well with studies conducted using cells adhered to hydrogel discs with diameters of centimeter scale.[25,28]

Further, unlike the cell adhesion hydrogels with dimensions of the centimeter scale, the use of hydrogel substrates with diameters of the micrometer to millimeter scales demonstrated the role the cell adhesion substrate curvature has on cellular activities. It is well known that shear stress controlled with flow rates regulates diverse cellular activities,

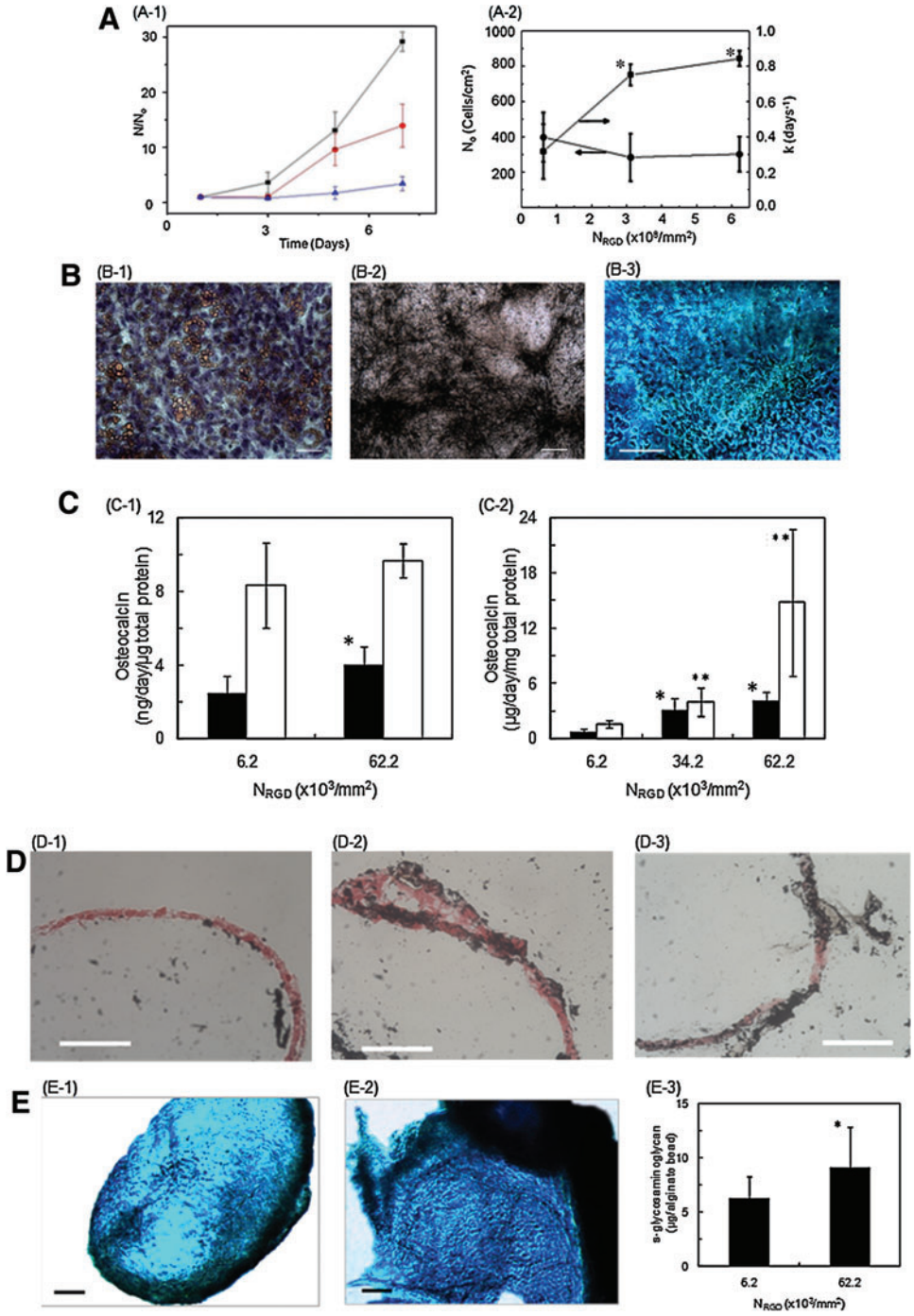

FIG. 2. Effect of RGD peptide density of of microgel (N_{RGD}) on MSC's proliferation and differentiation. The microgel diameter was kept constant at 500 μm. **(A)** (A-1) The dependency of MSC number (N) on cell culture period was controlled by RGD peptide density (N_{RGD}). The number of MSCs (N) was normalized to the number of cells adhered to the RGD-alginate microgels within first 24 h in culture (N_o). The N_{RGD} of the microgel surface was varied from 6.22×10^7 (▲) to 3.11×10^8 (●) and 6.22×10^8 RGD/mm^2 (■). (A-2) The N_0 (●) and the cell proliferation rate (k), (■) were significantly increased with N_{RGD}. The differences between the values were statistically significant. (*$p<0.05$). **(B)** The mesenchymal stem cells (MSCs) expanded on alginate microgels maintained multipotency. MSCs were isolated from the alginate microgels and re-seeded on poly(styrene) substrate. (B-1) MSCs cultured in adiopogenic media for 18 days were positively stained with Oil Red O (scale 100 μm). (B-2) MSCs cultured in osteogenic media for 18 days were positively stained for matrix mineralization with von Kossa reagents (scale 200 μm). (B-3) MSCs encapsulated in a collagen gel and cultured in chondrogenic media for 17 days were positively stained with Alcian blue **(C,** Scale: 150 μm**). (C)** Effects of N_{RGD} on MSC's osteogenic differentiation during cell culture in the osteogenic differentiation media. The extents of cellular osteocalcin secretion (C-1) and osteopontin secretion (C-2) were significantly higher for cells cultured on microgels with a higher RGD density (6.2×10^8 RGD/mm^2). The closed bar represents protein concentration measured at day 7 and the open bar represents that at day 14. The difference between the values was statistically significant (*$p<0.05$). **(D)** Increasing N_{RGD} increased the degree of mineralization on microgel surfaces, marked by positive staining with von Kossa reagents in black. The cells were counterstained in red. (D-1), (D-2) and (D-3) represent the microgel surfaces with N_{RGD} of 6.2×10^7 to 3.1×10^8 and 6.2×10^8 RGD/mm^2, respectively (scale bar: 100 μm). **(E)** Increasing N_{RGD} also elevated the chondrogenic differentiation level of MSCs cultured in the chondrogenic differentiation media. The glycosaminoglcan secreted by cells was positively stained by Alcian blue (Scale: 100 μm). (E-1) and (E-2) represent the microgel surfaces with N_{RGD} of 6.2×10^7 and 6.2×10^8 RGD/mm^2, respectively. The extent of quantified glycosaminoglycan production from cells on beads after 14 days in culture (E-3) (*$p < 0.05$). Color images available online at www.liebertonline.com/tea

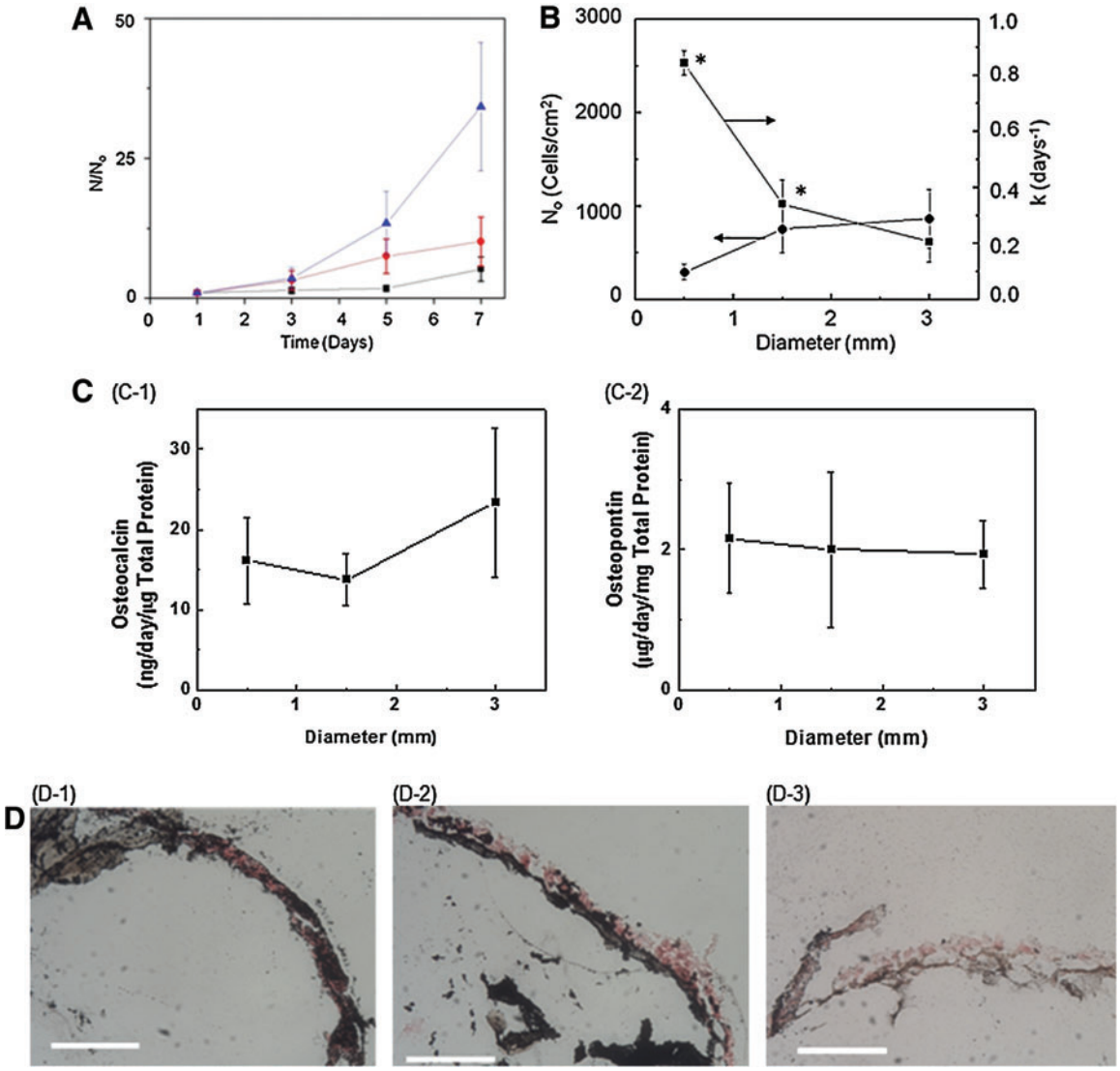

FIG. 3. Effect of microgel diameter on MSC's proliferation and differentiation. The N_{RGD} was kept constant at 6.22×10^8 N_{RGD}/cm^2. **(A)** The dependency of cell number (N) on cell culture period became larger with decreasing microgel diameter. The N was normalized to the number of cells adhered to the microgels within first 24 h of cell culture (N_o). The average diameter of the microgels were varied from 500 (▲) to 1500 (●) and 3000 μm (■). **(B)** Increasing the diameter of the alginate microgel significantly decreased the proliferation rate (k) (■), whereas it increased N_0 (●). The difference between values was statistically significant (*$p < 0.05$). **(C)** The degree of osteogenic differentiation of MSCs evaluated with measurements of the osteocalcin (C-1) and osteopontin (C-2) secretion levels after 7 days in culture showed no significant dependence on the microgel diameter. **(D)** The osteogenic differentiation of MSCs displayed by von Kossa staining was also independent of the diameter of the microgel and the cells were counterstained, shown in red. (D-1), (D-2), and (D-3) represent the microgel surfaces with diameter of 0.5, 1.5, and 3 mm, respectively (scale bar: 100 μm). Color images available online at www.liebertonline.com/tea

including cell growth. According to simulation, the cell adherent microgels continuously rotate with convective flow in a bioreactor and the wall shear stresses acting on the microgel surfaces change with the microgel diameter. Therefore, the magnitude of shear stress, which acted on the cells, should be mediated by the microgel curvature.[29] The range of the shear stresses altered with the microgel diameter falls within a range of shear stresses known to influence activities of cells adhered onto a flat 2D substrate.[30–32] Therefore, it is proposed that the smaller microgel amplified effects of shear stress on reducing the cell attachment and stimulating the cell growth even at a given flow rate.[33] The benefit of culturing cells on smaller microgels most likely reaches an endpoint because microcarriers with diameters smaller than 100 μm limit cell adhesion to their surfaces.[34]

In addition, the larger dependency of the cell growth rate on the microgel diameter than the dependency of cell differentiation implies that cells at confluency for the differentiation assay were less sensitive to the changes of shear stress, as also confirmed with independency of differentiation level on the direct change of shear stress. It has been known that increased cell–cell contacts leads to the decrease of the cellular sensitivity to the shear stress.[35] This is why our result is different from previous studies that report the critical role of shear stress in stimulating osteogenic differentiation using cells laden into a 3D microporous scaffold or

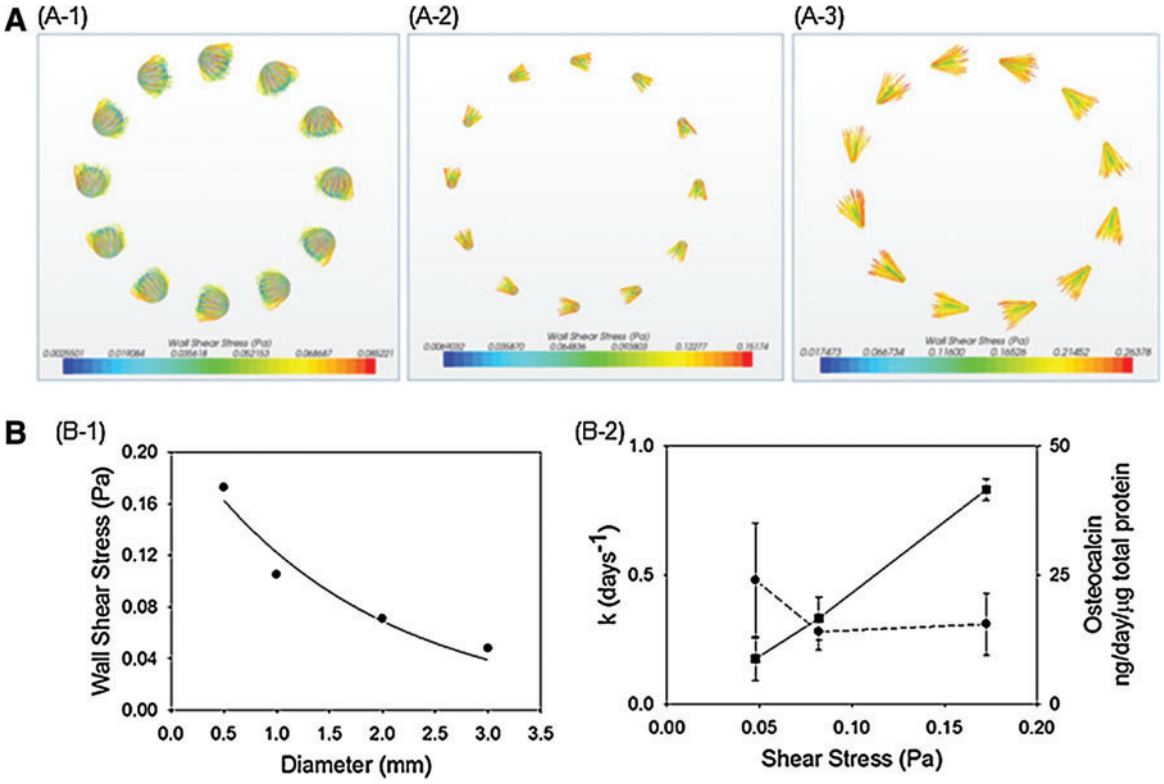

FIG. 4. Numerical analysis of the effect of microgel diameter on shear stress over microgel surfaces. **(A)** Computational fluid dynamics simulations were implemented to calculate the wall shear stresses acting on cells adhered to the microgel with controlled diameters from (A-1) 3 mm, to (A-2) 1.5 mm, and (A-3) 0.5 mm. **(B)** (B-1) The average wall shear stresses acting on the microgels increased as the microgel diameter decreased. (B-2) The proliferation rate (k) (■) of MSCs was increased with shear stresses acting on the cells, whereas osteogenic differentiation levels (●) of MSCs were independent of the shear stresses. Color images available online at www.liebertonline.com/tea

those plated on a substrate at a density to limit cell–cell contacts. The magnitudes of cellular signaling activations altered by the microgel curvature and their relevance to cell growth and differentiation should be further analyzed in future studies.

Conclusion

Taken together, the results of this study present a rational design of a microgel that can potentially serve as a cell adhesion substrate enabling large-scale multipotent cell culture. The chemical linkage of the RGD peptides to the microgel enabled the control of MSC growth rate and differentiation level with the RGD peptide density, likely because of the change of the number of bonds between cellular integrin and RGD peptides. At a given RGD peptide density, the microgel diameter also influenced the MSC growth rate, because shear stresses acting on the cells were changed with microgel curvature. Overall, the results of this study will provide valuable guidelines to designing a broad array of advanced microcarriers used for the large scale cell culture. Thus, multipotent cells may be cultured in a controllable and predictable manner independent of the scale-up of a cell culture, which may expedite use of these cells in clinical settings. Furthermore, this finding will be also useful to designing an implantable cell adherent microcarrier used in various cell therapies, including tissue regeneration therapy.

Acknowledgments

The authors thank the American Heart Association (0830468Z) and National Institute of Health (NIH 1 R21 HL097314A) for financial support of their research, Dr. Frank Rauh at FMC Biopolymer for the generous supply of alginate, and Jongkoo Lim at GS Caltex for support in performing the modeling work and use of workstations.

Disclosure Statement

No competing financial interests exist.

References

1. Aversa, F., Tabilio, A., Velardi, A., Cunningham, I., Terenzi, A., Falzetti, F., *et al.* Treatment of high-risk acute leukemia with T-cell-depleted stem cells from related donors with one fully mismatched HLA haplotype. N Engl J Med **339,** 1186, 1998.
2. Gratwohl, A., Hermans, J., Goldman, J.M., Arcese, W., Carreras, E., Devergie, A., *et al.* Risk assessment for patients with chronic myeloid leukaemia before allogeneic blood or marrow transplantation. Lancet **352,** 1087, 1998.
3. Jaiswal, N., Haynesworth, S.E.,Caplan, A.I., and Bruder, S.P. Osteogenic differentiation of purified, culture-expanded human mesenchymal stem cells *in vitro*. J Cell Biochem **64,** 295, 1997.
4. Perin, E.C., Dohmann, H.F.R., Borojevic, R., Silva, S.A., Sousa, A.L.S., Mesquita, C.T., *et al.* Transendocardial,

autologous bone marrow cell transplantation for severe, chronic ischemic heart failure. Circulation **107,** 2294, 2003.
5. Pittenger, M.F., Mackay, A.M., Beck, S.C., Jaiswal, R.K., Douglas, R., Mosca, J.D., *et al.* Multilineage potential of adult human mesenchymal stem cells. Science **284,** 143, 1999.
6. Siepe, M., Heilmann, C., von Samson, P., Menasche, P., and Beyersdorf, F. Stem cell research and cell transplantation for myocardial regeneration. Eur J Cadiothorac Surg **28,** 318, 2005.
7. Toma, C., Pittenger, M.F.,Cahill, K.S., Byrne, B.J., and Kessler, P.D. Human mesenchymal stem cells differentiate to a cardiomyocyte phenotype in the adult murine heart. Circulation **105,** 93, 2002.
8. Zittoun, R.A., Mandelli, F., Willemze, R., Dewitte, T., Labar, B., Resegotti, L., *et al.* Autologous or allogeneic bone-marrow transplantation compared with intensive chemotherapy in acute myelogenous leukemia. N Engl J Med **332,** 217, 1995.
9. Aebischer, P., Wahlberg, L., Tresco, P.A., and Winn, S.R. Macroencapsulation of dopamine-secreting cells by coextrusion with an organic polymer-solution. Biomaterials **12,** 50, 1991.
10. Bautz, F., Rafii, S., Kanz, L., and Mohle, R. Expression and secretion of vascular endothelial growth factor-A by cytokine-stimulated hematopoietic progenitor cells: possible role in the hematopoietic microenvironment. Exp Hematol **28,** 700, 2000.
11. Caplan, A.I. Adult mesenchymal stem cells for tissue engineering versus regenerative medicine. J Cell Physiol **213,** 341, 2007.
12. Riha, G.M., Lin, P.H., Lumsden, A.B.,Yao, Q.Z., and Chen, C.Y. Application of stem cells for vascular tissue engineering. Tissue Eng **11,** 1535, 2005.
13. Lock, L.T., and Tzanakakis, E.S. Stem/progenitor cell sources of insulin-producing cells for the treatment of diabetes. Tissue Eng **13,** 1399, 2007.
14. Botchwey, E.A., Pollack, S.R., Levine, E.M., and Laurencin, C.T. Bone tissue engineering in a rotating bioreactor using a microcarrier matrix system. J Biomed Mater Res **55,** 242, 2001.
15. Malda, J., Kreijveld, E., Temenoff, J.S.,van Blitterswijk, C.A., and Riesle, J. Expansion of human nasal chondrocytes on macroporous microcarriers enhances redifferentiation. Biomaterials **24,** 5153, 2003.
16. Qiu, Q.Q., Ducheyne, P., and Ayyaswamy, P.S. 3D Bone tissue engineered with bioactive microspheres in simulated microgravity. In Vitr Cell Dev Biol Anim **37,** 157, 2001.
17. Xu, T., Li, S.L., Pan, J.L., and Yu, Y.T. Preparation and hepatocyte culture on agar-based microcarriers. Chem J Chin Univ **20,** 1230, 1999. [In Chinese.]
18. Zhu, X.H., Tabata, Y., Wang, C.H., and Tong, Y.W. Delivery of Basic Fibroblast Growth Factor from Gelatin Microsphere Scaffold for the Growth of Human Umbilical Vein Endothelial Cells. Tissue Eng Part A **14,** 1939, 2008.
19. Kong, H.J., Polte, T.R., Alsberg, E., and Mooney, D.J. FRET measurements of cell-traction forces and nano-scale clustering of adhesion ligands varied by substrate stiffness. Proc Natl Acad Sci U S A **102,** 4300, 2005.
20. Kong, H.J., Boontheekul, T., and Mooney, D.J. Quantifying the relation between adhesion ligand-receptor bond formation and cell phenotype. Proc Natl Acad Sci U S A **103,** 18534, 2006.
21. Engler, A.J., Sen, S., Sweeney, H.L., and Discher, D.E. Matrix elasticity directs stem cell lineage specification. Cell **126,** 677, 2006.
22. Shiragami, N., Honda, H., and Unno, H. Anchorage-dependent animal-cell culture by using a porous microcarrier. Bioprocess Eng **8,** 295, 1993.
23. Dellatore, S.M., Garcia, A.S., and Miller, W.M. Mimicking stem cell niches to increase stem cell expansion. Curr Opin Biotechnol **19,** 534, 2008.
24. King, J.A., and Miller, W.M. Bioreactor development for stem cell expansion and controlled differentiation. Curr Opin Chem Biol **11,** 394, 2007.
25. Rowley, J.A., Madlambayan, G., and Mooney, D.J. Alginate hydrogels as synthetic extracellular matrix materials. Biomaterials **20,** 45, 1999.
26. Kong, H.J., Kim, C.J., Huebsch, N., Weitz, D., and Mooney, D.J. Noninvasive probing of the spatial organization of polymer chains in hydrogels using fluorescence resonance energy transfer (FRET). J Am Chem Soc **129,** 4518, 2007.
27. Bancroft, G.N.,Sikavitsast, V.I.,van den Dolder, J., Sheffield, T.L., Ambrose, C.G., Jansen, J.A., *et al.* Fluid flow increases mineralized matrix deposition in 3D perfusion culture of marrow stromal osteloblasts in a dose-dependent manner. Proc Natl Acad Sci U S A **99,** 12600, 2002.
28. Hsiong, S.X., Carampin, P., Kong, H.J., Lee, K.Y., and Mooney, D.J. Differentiation stage alters matrix control of stem cells. J Biomed Mater Res Part A **85A,** 145, 2008.
29. Stolberg, S., and McCloskey, K.E. Can shear stress direct stem cell fate? Biotechnol Prog **25,** 10, 2009.
30. Croughan, M.S., Hamel, J.F., and Wang, D.I.C. Hydrodynamic Effects on animal-cells grown in microcarrier cultures. Biotechnol Bioeng **29,** 130, 1987.
31. Kreke, M.R., and Goldstein, A.S. Hydrodynamic shear stimulates osteocalcin expression but not proliferation of bone marrow stromal cells. Tissue Eng **10,** 780, 2004.
32. Pavalko, F.M., Chen, N.X., Turner, C.H., Burr, D.B., Atkinson, S., Hsieh, Y.F., *et al.* Fluid shear-induced mechanical signaling in MC3T3-E1 osteoblasts requires cytoskeleton-integrin interactions. Am J Physiol Cell Physiol **275,** C1591, 1998.
33. Park, J.S., Huang, N.F., Kurpinski, K.T., Patel, S., Hsu, S., and Li, S. Mechanobiology of mesenchymal stem cells and their use in cardiovascular repair. Front Biosci **12,** 5098, 2007.
34. Zhou, W., Seth, G., Guardia, M.J., Hu, W.-S., and Flickinger, M.C. Mammalian Cell Bioreactors. Hoboken, NJ: John Wiley & Sons, Inc., 2009.
35. Motobu, M., Wang, P.C., and Matsumura, M. Effect of shear stress on recombinant Chinese hamster ovary cells. J Ferment Bioeng **85,** 190, 1998.

Address correspondence to:
Hyunjoon Kong, Ph.D.
Department of Chemical and Biomolecular Engineering
University of Illinois at Urbana-Champaign
Urbana, IL 61801-3602

E-mail: hjkong06@illinois.edu

Received: November 25, 2010
Accepted: June 15, 2011
Online Publication Date: July 22, 2011